



An Improved Grey Wolf Optimization–Based Convolutional Neural Network for the Segmentation of COVID-19 Lungs–Infected Parts

P. Sridhar¹ · Jayaraj Ramasamy² · Ravi Kumar³ · Ramakrishnan Ramanathan⁴ · Rakesh Nayak⁵ · M. Tholkapiyan⁶

Received: 24 June 2022 / Accepted: 30 July 2023 / Published online: 12 August 2023
© The Author(s), under exclusive licence to Springer Science+Business Media, LLC, part of Springer Nature 2023

Abstract

The coronavirus outbreak is a recent pandemic that destroyed most of the lives, economy, and livelihoods. The detection of COVID-19 is the main aim to detect and provide better treatment for patients to mitigate its impact. In addition, it is necessary to diagnose the disease swiftly with upgraded technologies. This can be achieved by CT image scanning. This provides the fastest detection of the disease. Moreover, it can also be used to diagnose the percentage of the affected lung areas. To perform this fastly, we propose a novel approach known as Convolutional Neural Network (CNN)–based Improved Grey Wolf Optimization (IGWO) algorithm. The proposed CNN utilizes a SegNet-based approach which can be used to detect the affected area in the lungs by using the encoder and decoder steps. The encoder in this approach uses three types of CNN architecture. First, the decoder is used to reconstruct the images. The overfitting issues during the iterations and complexities are reduced by adopting the IGWO approach. The experimental analysis depicts that the proposed approach effectively segments the CT images and promptly diagnoses the affected lung area.

Keywords COVID-19 · Segmentation · Grey wolf optimization · Statistical noises · CT images · Convolutional neural network

Introduction

Recently, a coronavirus is discovered in China, commonly known as Severe Acute Respiratory Syndrome Coronavirus [1]. It can spread fast, affecting 217 countries and territories

worldwide and affecting the respiratory system [2]. The symptoms of this virus are cough, cold, fever, and breathing problems. The respiratory system and lungs are affected by this coronavirus. According to death and the total number of cases, the World Health Organization mentioned this virus as a global public health emergency [3]. To control the spread of the virus, self-isolation, social distancing, and quarantining are the steps taken by every individual. This pandemic situation affects the economic crisis, pressure, and resources.

Currently, people are affected by different domains due to economic conditions. Finance is a significant problem for countries and individuals in health facilities. The X-rays and the CT scan are the requirements to identify the severity of the diseases in the lungs. Artificial Intelligence is applicable in medical measures, and numerous COVID-19 cases are monitored and recorded. Due to severe attacks, the lungs are affected and cause death. The infections are monitored and accessed through various methods to diagnose accurate data [4].

In biomedical engineering, AI assists the severity of coronavirus in evaluating the efficiency and accuracy [5, 6], to enhance the deep learning approaches applied to determine the COVID-19 persons. The performance of the image is executed in the image processing to perform the images [7, 8]. A CAT scan is also known as computed tomography; the

✉ P. Sridhar
psridhar525@gmail.com

¹ Department of Electrical and Electronics Engineering, Institute of Aeronautical Engineering, 500043 Hyderabad, Telangana, India

² Department of IT, Botho University, Gaborone, Botswana

³ Department of Electronics and Communication Engineering, Jaypee University of Engineering and Technology, Guna 473226, India

⁴ Department of IT, Vignan's Foundation for Science, Technology & Research (Deemed to be University), Guntur Dist. AP 522 213 Vaddlamudi, India

⁵ Department of CSE, O P Jindal University, 496109 Punjipathra, Raigarh, Chattisgarh, India

⁶ Department of Civil Engineering, Saveetha School of Engineering, Saveetha Institute of Medical and Technical Sciences (SIMATS), 602105 Chennai, Tamil Nadu, India

input is given as an image and output feature. It has enormous images to remodel the 3-dimensional appearance. Machine learning collects the image automatically to identify a set of data. In Artificial Intelligence, the data is designed to achieve certain goals. It solves the obstacles of the machine and deep learning methods. It automatically reduces the size and result of the specific data. However, it does not compute the correct data due to complexity and expense.

Meanwhile, image segmentation faces challenges due to the images' low contrast, illumination, and irregularity [9]. Segmentation is nothing but dividing the various parts into various parts that relies on the same properties of the neighboring pixels. Several machines and deep learning approaches are worked in this field, such as Support Vector Machines [10], Convolutional Neural Networks [11, 12], and Deep Neural Networks [13]. The existing works do not provide correct accuracy and increase computational time. However, optimized segmentation is still required due to the increased complexity. Hence to overcome these issues, we proposed a novel approach known as the CNN-IGWO approach, which is effectively used to segment the COVID-19-affected parts of the lungs. The average segmentation time for lung parenchyma areas using the suggested CNN model is calculated to be 10.75 s for each slice of 512,512 voxels or pixel-wise segmentation. Using a machine with numerous cores or a GPU helps speed up the computation. Facilitate image analysis, which entails segmenting a visual input. Sets of one or more pixels make up segments. Image segmentation divides pixels into more substantial parts while simultaneously doing away with the requirement to treat each pixel as a separate unit.

The key points of our work are listed below.

- The collected data are normalized by the Z-score approach to remove the unwanted noises due to the distraction and low resolution.
- The SegNet-based CNN is used to segment the CT images and effectively group the features.
- The Encoder in the SegNet extracts the features and converts them into low-resolution features. Finally, the decoder is used to reconstruct the encoded images.
- Then, the results are optimized using the GWO approach, which effectively chooses the features globally. It also can be used to overcome the overfitting issues in the SegNet-based CNN approach.

The rest of the article is organized as follows: in the “[Literature Survey](#)” section, the relevant works are analyzed with their advantages and disadvantages. The proposed methodology is explained in the “[Proposed Methodology](#)” section. The experimental analysis is illustrated in the “[Experimental Investigation and Analysis](#)” section. Finally, the article is summarized in the “[Conclusion](#)” section.

Literature Survey

Some of the Literatures Related to the Presented Work are Listed Below

To partition the infected and non-infected patients, Castiglione et al. [14] have proposed an Automatic Detection of Coronavirus optimized CNN (ADECO-CNN), to examine the CT images faster for the analysis of COVID-19. The normalization method increases the quality and removes noise from lung images. Radiography and CTs are used as the patterns, and it is derived from websites and X-rays. It can perform real-time classification of diseases. Nonetheless, it should be developed for similar diseases.

Castiglione et al. [15] have described the sensors to identify the persons infected with COVID-19 based on IoT devices. The structure consists of a data warehouse, health centers, and so on. The information is detained from different COVID-19 patients. The IoT devices use sensors in the diagnosis of the health of the patients. It can be able to control the situation in a short period. As a result, the COVID-19 patients are cured in a limited period. Thus, the IoT is used correctly in the decision-making process.

Vahdat et al. [16] have stated Loading Aware Training Invertor Memristive (LATIM) determines the size to precise the coefficients. The training neurons determine the invertor's size. The c and d are the coefficients of training data. The output value of the training network is efficient. To determine the training values of conductance, the memristors are predicted. The neural networks function as the investors to generate, although the complexity should have been improved.

A portable healthcare tool, Kaiser et al. [17] have discussed iWork Safe to detect COVID-19 patients. The mobile app is used to check and monitor infected persons. The fuzzy neural network measures fitness. The method that is evaluated is to monitor the health condition. In critical situations, the app is trained by data. The quality should be high to function the app. Thus, the machine learning approach is extended in future work.

Aradhya et al. [18] introduced a chest X-ray to investigate COVID-19-infected people. The phase-to-phase approach is very efficient in detecting images. Probabilistic Neural Networks (PNN) are applicable in large datasets. From each data, the image is selected to compute the distributions. The entropy is more effective in selecting images. The formatted images are collected in a different database. Thus, the data should be improved from different fields.

Mahmud et al. [19] studied briefly about COVID-19 Tri-level Attention Network (CovTANet). This method divides the segments to form volumes. Positive false estimations lose the data. The divided data is extracted to employ the task. The features are extracted from different regions to divide the vectors. The segments are improved to optimize

the problems in relevant features. As a result, the damages are reduced in a faster response, even though the method in the neural network should be productive.

To segment COVID-19, Mahmud et al. [20] stated a novel approach known as CT volumes to limit the neural network. The encoder and decoder are integrated to increase the module. The 2D network is extracted from the 3D network. It has been used to demonstrate the sliced data to extract the CT volumes. The complexity is reduced to improve the volumes. Moreover, the task is performed in multi-class segments.

A multi-task deep learning-based technique for lung infection segmentation on CT scan images was presented by Elharrouss et al. in 2022 [21]. Segmenting the potential infection-prone lung areas is the first step in our suggested procedure. Additionally, the suggested model is trained using the two-stream inputs to execute a multi-class segmentation. Thanks to the multi-task learning approach, we can get around this work's lack of labeled data. The multi-input stream also enables the model to benefit from various features that can enhance the outcomes. The proposed technique, which shows success for lung infection segmentation, reached 78.6% for dice, 71.1% for sensitivity measure, 99.3% for specificity, 85.6% for precision, and 0.062 for average absolute error metric.

Fan et al. [22] presented a unique COVID-19 Lung Infection Segmentation Deep Network (Inf-Net) to detect infected regions from chest CT slices in 2020 automatically. Using a parallel partial decoder, our Inf-Net combines high-level characteristics to create a world map. The boundaries are then modeled, and the representations are improved via explicit edge attention and implicit reverse attention. Additionally, we provide a semi-supervised segmented framework built on a randomly chosen propagation approach to address the lack of labeled data. This framework only needs a small number of labeled photos and mostly uses unlabeled data. Numerous tests using our COVID-SemiSeg and actual CT volumes show that the suggested Inf-Net surpasses most cutting-edge specific limitations and improves performance.

Proposed Methodology

This section presents our proposed SegNet-CNN-based IGWO approach for segmenting the COVID-19-affected part of the lungs. First, the collected images are normalized to remove the statistical noises and then fed into the proposed work. Figure 1 illustrates the proposed approach in a detailed manner.

Image Normalization

Z-score normalization is a common approach widely used in computer vision applications for image pre-processing. It

is deployed to normalize the image pixel values to have zero mean and unit variance; thus, it enhances the image quality. This step is performed to remove the statistical noises present in the lungs' CT images. The statistical noises are divided into three types: (i) electrical equipment that causes unnecessary interference to lead to electronic noise, (ii) noise that occurs while reconstructing the images in the receiver coils, and (iii) stochastic noise, which is the main source of noises [23]. This type of noise can be ignored by increasing the number of photons. Maintaining the tradeoff between image resolution quality and radiation risk is necessary. Before the segmentation process, removing the noises from the acquired CT images of the lungs is necessary. This can be achieved by the image normalization approach, which can be used to smooth the images and enhance the contrast of the images near the border of the lungs.

The image pre-processing using the Z-score normalization involves conversion of image to gray scale, mean and standard deviation calculation, normalization of pixel values, and scaling of pixel values. Initially, the color image is converted to gray scale to shorten the normalization process. Then, the mean and standard deviation of the image pixel values are determined. In pixel value normalization, the estimated mean is subtracted from each pixel value and the result is divided by the standard deviation. This confirms that the pixel values have zero mean and unit variance. Finally, the pixel values are scaled to a desired range (between 0 and 1 or between -1 and 1). The utilization of Z-score normalization enhances the system performances by eliminating the lighting effects and contrast variations in the image. Our proposed approach utilizes the Z-score normalization method, which provides unit variance and zero mean for the nonzero values of the images [24]. The Z-score normalization is formulated as,

$$Z = \frac{(b - \tau)}{\lambda} \quad (1)$$

Here, the mean and standard deviation are given as τ and λ respectively. The intensity of the current pixel can be given as b . The resultant output is illustrated in Fig. 2. The original CT images are illustrated in the first column of Fig. 1. The second column represents the output of the Z-score normalization. From the figure, effective detection is achieved by our proposed method by detecting the borders of the lungs without the inclusion of lesions. The resultant outputs are then segmented using the proposed CNN-based IGWO approach. The following sections elucidate the proposed approach.

SegNet-Based CNN

Our proposed work utilizes the SegNet-based CNN technique [25]. SegNet has two parts: (i) encoder and (ii) decoder. The proposed CNN utilizes a SegNet-based

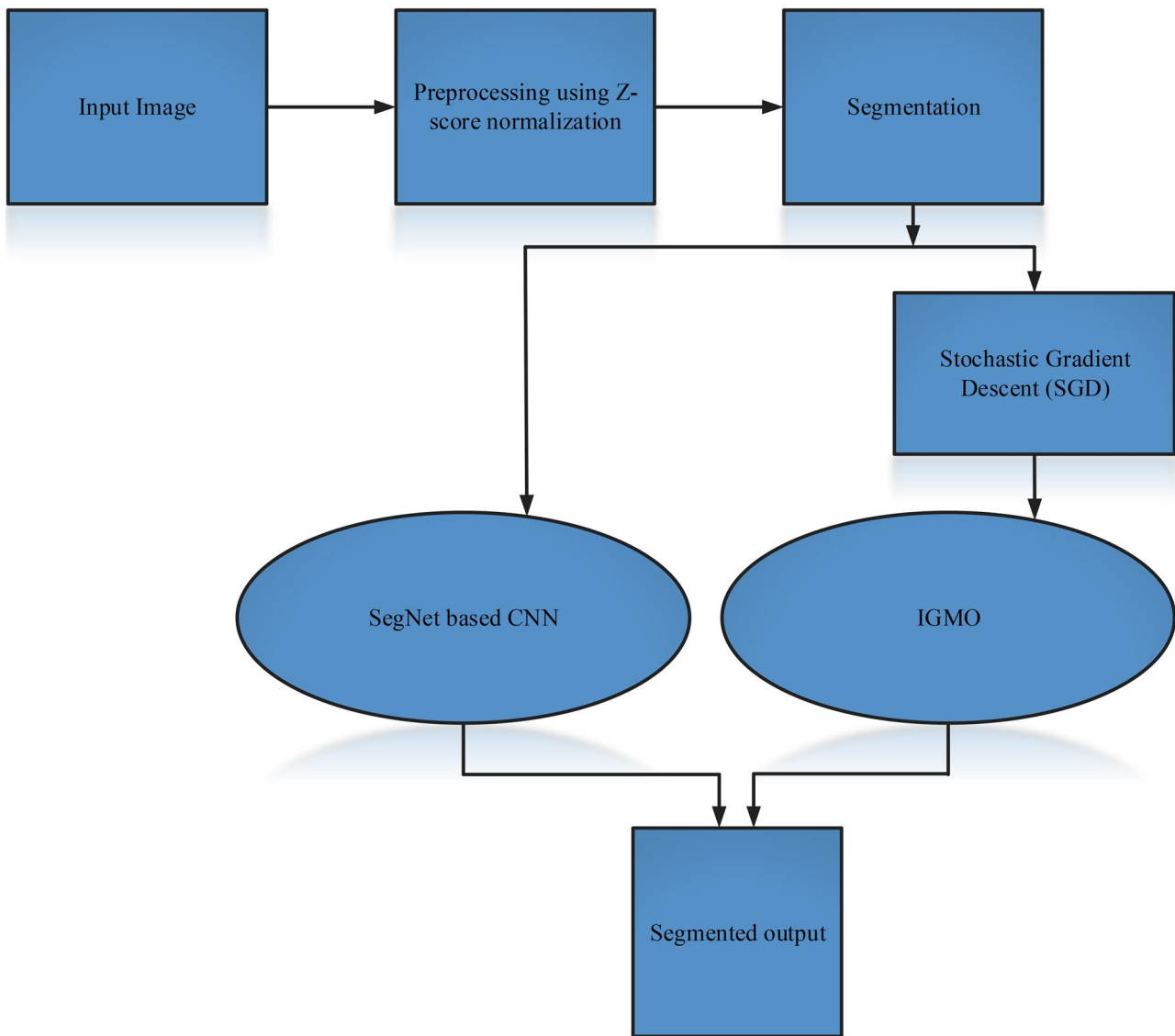
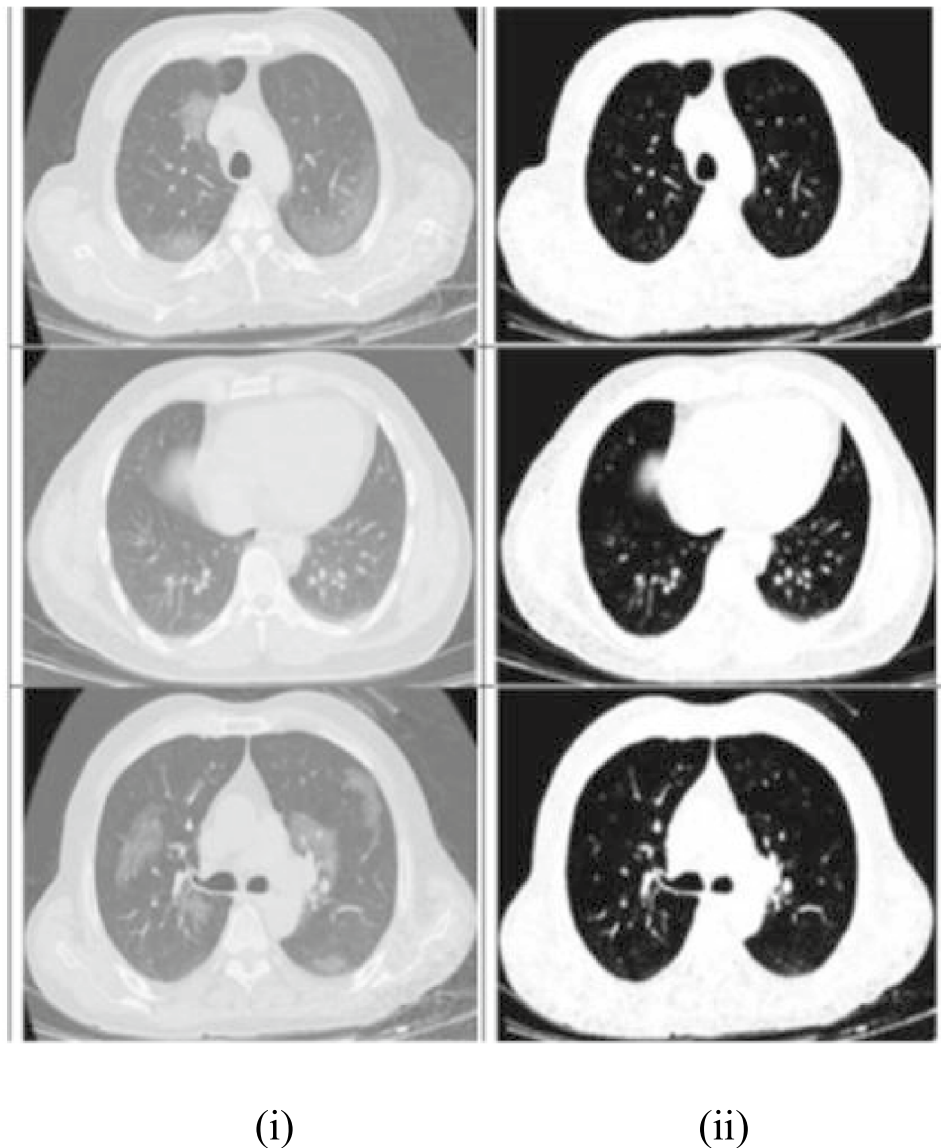


Fig. 1 Parts of the proposed methodology portion

approach which can be used to detect the affected area in the lungs by using the encoder and decoder steps. SegNet is a type of Convolutional Neural Network (CNN) structure that is commonly utilized in image processing for segmentation purposes. This involves transforming each pixel in an image to a specific class [26]. The SegNet infrastructure includes encoder and decoder networks, which works together to perform image segmentation task. The encoder network takes an input image and passes through a convolutional and pooling layers sequence. These layers track and extract essential features at multiple scales. Furthermore, the output of each layer is passed to the equivalent layer in the decoder link. The decoder network utilizes convolutional and upsampling layers to provide a pixel-wise

segmentation map. In addition, the SegNet uses the pooling indices from the encoder to achieve accurate upsampling in the decoder net, enabling the system to preserve fine-grained information in the segmentation map. Moreover, it minimizes the number of parameters in the network, making it more efficient than other segmentation techniques [27, 28]. Furthermore, the SegNet model can handle complex lung structures like airways and blood vessels. Moreover, the flexibility of the SegNet enables the system to train various types of medical images like CT and MRI, making it a suitable architecture for medical image processing tasks. Thus, the encoder-decoder architecture in the SegNet enables the model to extract the lung tissue's contextual information and spatial dependencies. These advantages in the SegNet enable

Fig. 2 Outcome of image normalization process. **i** Original images. **ii** Normalized output



us to perform the lung segmentation task more effectively than the other networks like U-Net and DeepLab.

- Encoder:** It is exploited to extract the required features from the normalized CT images. It is composed of convolutional and max-pooling layers of VGG16 [29], VGG19 [30], and ResNet50 [31]. The convolutional layers perform feature extraction by applying a sequence of filters to the image. On the other hand, the pooling layers minimize the spatial dimensions of the output by considering the highest value in each pooling region. Finally, the result of each layer is made to pass through the non-linear activation function to provide non-linearity in the system. Figure 3 illustrates the encoder model. It can also be used to provide an activation map with a low resolution even though it carries entire image data information. It is also used to save the data needed for decoding purposes.
- Decoder:** The decoder network accepts the output of the last layer of the encoder network and utilizes it to provide a pixel-wise segmentation map. It is used to reconstruct the CT images from the extracted features by the encoder, i.e., by the activation map low-resolution information. The second part of Fig. 2 illustrates the decoder of SegNet. The upsampling process of the decoder can enhance the resolution of the activation map obtained from the encoder. Upsampling layers are available in the decoder, which performs the inverse pooling operation. The upsampling layers enhance the spatial dimensions of the image by iterating the pixel values in each upsampling region. The convolutional layers perform feature mapping by applying filters to the upsampled image. The upsampling and max-pooling operations are depicted in Fig. 3. The max-pooling layers are used to mitigate the activation map and cache the maximized indices values

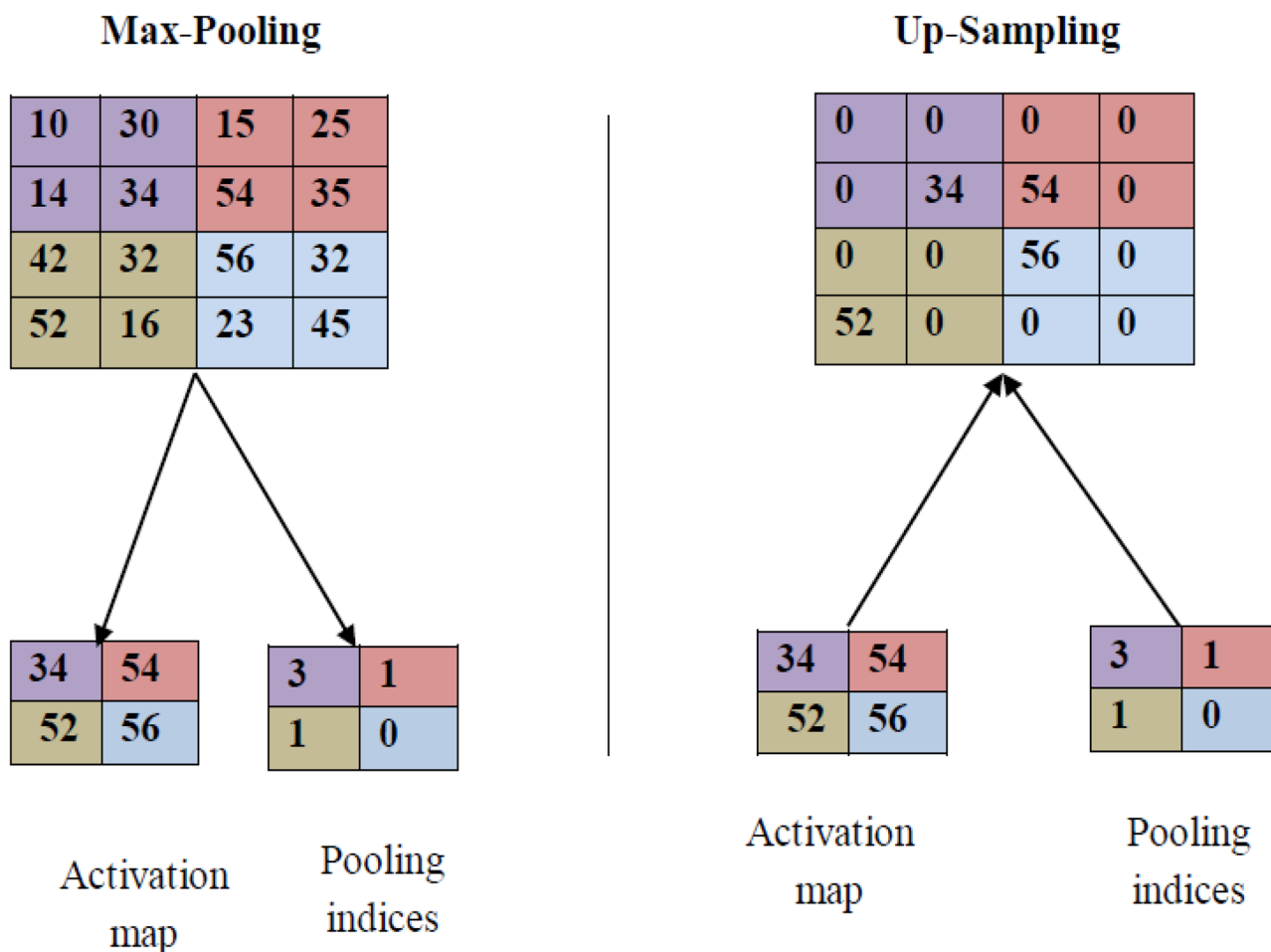


Fig. 4 Sample of max-pooling and upsampling process

$$A_j^k(t + 1) = A_r^k(t) - R * |A_r^k(t) - A_{j(t)}^k| \tag{6}$$

$A_{j(t)}^k$ is the solution of the wolf at the t^{th} iteration; the j^{th} solution at the dimensionality of k . Subsequently, the optimal local solution can be estimated $|R| > 1$ at the interval that lies between -2 and 2 . Then, the ability of prey to search and attack can be given as $|R| > 1$ and $|R| < 1$. The newly updated location beyond the constraints is given in Eq. (6). The constraints are set by using the original GWO. This might have exceeded the constraints by arbitrary locations [34].

$$A_j^k(t + 1) = \begin{cases} A_j^k(t) + f * (E^k - A_j^k(t)), & \text{if } A_j^k(t + 1) > E^k \\ A_j^k(t) + f * (L^k - A_j^k(t)), & \text{if } A_j^k(t + 1) > L^k \end{cases} \tag{7}$$

The upper and lower constraints are given as E^k and L^k . F is the random integer and lies between the values 0 and 1. Finally, the capability of the random walk and behaviors is analyzed by using random movement.

Proposed SegNet-CNN-Based IGWO Approach for the Segmentation of COVID-19-Infected Parts

The proposed approach initializes the parameters of both techniques. At first, the sample images from the dataset are trained, and then the images are passed to the data normalization process. Consequently, the normalized images are segmented by using the SegNet-based CNN. Furthermore, the overfitting issues during the iterations and complexities are reduced by adopting the IGWO approach. Finally, the output obtained is optimized using the IGWO approaches, which are explained in Fig. 5.

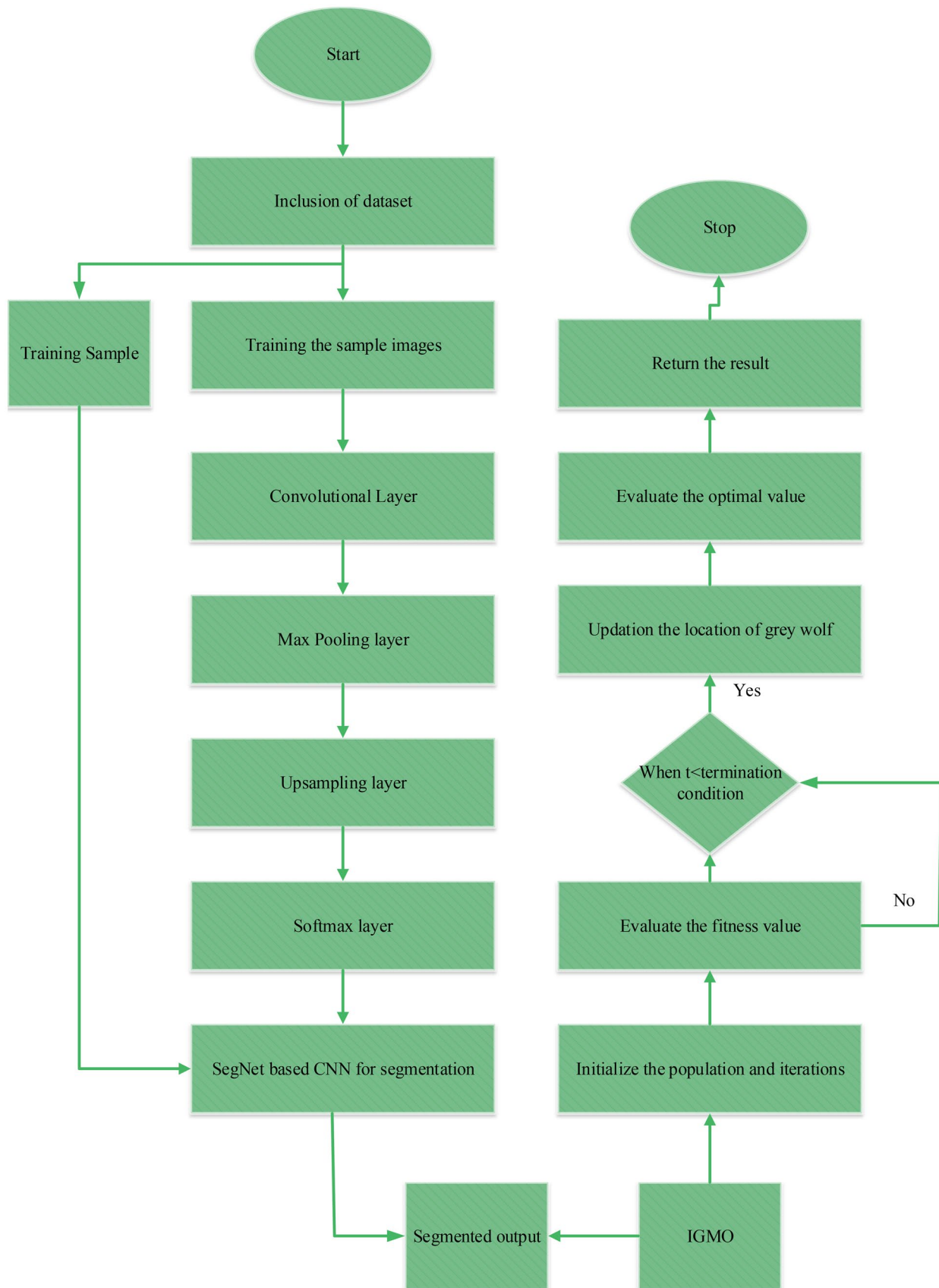


Fig. 5 Schematic overlay of the proposed approach

Experimental Investigation and Analysis

This section discusses the experimental evaluation of the proposed methodology. For the experimental purpose, we used Windows 10 (64-bit) operating system, with the Intel(R) RAM with the speed of Core(TM) i7-3.4 GHz + GEFORCE GTX 1080 Ti GPU + 16 gigabytes with the experiments running on the Python platform [35] and [36]. Table 1 explains the parametric values of the proposed framework. The experimental analysis depicts that the proposed approach effectively segments the CT images and thereby promptly diagnoses the affected area in the lungs.

Dataset Explanation

The existing studies with the proposed methodology performance are validated via various performance measures to estimate the experimental accuracy, validity, and reliability. The borders are manually segmented and accurately section the corrupted tissues. This is important to note that using an enhancement approach to expand the volume of data results in a maximum number of new samples. Moreover, 70% of the total data can be utilized for learning, 10 percentage points for verifying, and 20% for the test. Information augmentations effectively reduce errors in training and validation [37].

The augmentation methods use data upsampling or bending to try and boost the training dataset size. The previous image labels are kept during the process of augmentation, which is known as augmentations of data distortion. This model comprises neural style transfer, random erasing, adversarial training, geometric transformations, and color. The training set adds this, and the synthetic samples are generated via oversampling augmentations [38]. This study utilized six data augmentation methods to enhance random erasing, color space transformations, noise injection, translation, rotation, color space, and flipping. We used horizontal axis flipping during flipping and employed contrast enhancement in the color space [39]. Select 180° rotation and then apply up, down, left, and right in translation. Utilize the Gaussian distribution in the noise rejection. Apply the constant value to increase and decrease the pixel values in color space transformations. Finally,

Table 1 Parametric values

Parameters	Ranges
Number of convolutional layers	7
Activation function	Softmax
Population size	50
Maximum number of iterations	200

randomly select the $n \times m$ image patch in random erasing. The segmented sample images based on the proposed method are delineated in Table 2.

Result and Discussion

The performance metrics dice similarity (D), volume overlap error (V), maximum surface distance (MSD), root mean square symmetric surface distance (RMSD), average surface distance (ASD), relative volume difference (RVD), *F*-score, precision, recall, and accuracy are used. This investigation was performed among various methods, such as ADECO-CNN [14], PNN [18], MT-DL [21], Inf-Net [22], and the proposed method.

Performance Metrics

The proposed model efficiency is calculated and compared using various performance measures. The evaluation measures, namely dice similarity (D), volume overlap error (V), maximum surface distance (M_{SD}), root mean square symmetric surface distance (R_{MSD}), average surface distance (A_{SD}), relative volume difference (R_{VD}), *F*-score, precision, recall, and accuracy, are used.

$$AUC = \frac{1}{2} \left(\frac{T_p}{F_n + T_p} + \frac{T_n}{F_p + T_n} \right) \tag{8}$$

$$Accuracy = \frac{T_n + T_p}{F_n + T_n + T_p + F_p} \times 100 \tag{9}$$

$$Precision = \frac{T_p}{T_p + F_p} \tag{10}$$

$$Recall = \frac{T_p}{F_n + T_p} \tag{11}$$

where T_p and T_n are the true positive and true negative classes; the false positive and negative classes are F_p and F_n [36–38].

$$V(N_{S1}, N_{S2}) = \left(1 - \frac{N_{S1} \cap N_{S2}}{N_{S1} \cup N_{S2}} \right) \times 100\% \tag{12}$$

$$D = \left(2 \times \frac{T_p}{2 \times T_p + F_n + F_p} \right) \times 100\% \tag{13}$$

$$A_{SD} = \frac{1}{|C_{N_{S1}}| + |C_{N_{S2}}|} \times \left(\sum_{y \in C_{N_{S1}}} e(y, C_{N_{S2}}) + \sum_{y \in C_{N_{S2}}} e(y, C_{N_{S1}}) \right) \tag{14}$$

Table 2 Segmented sample images based on the proposed method

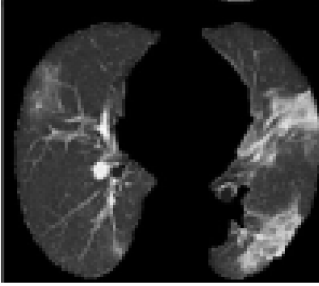
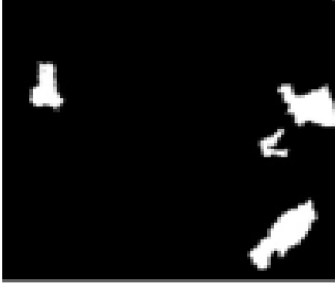

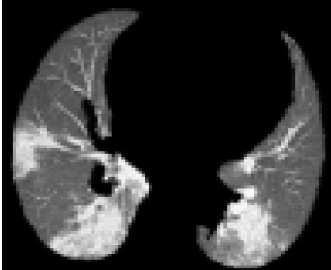
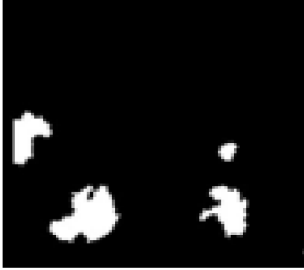

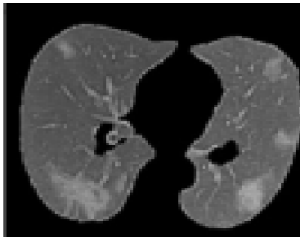

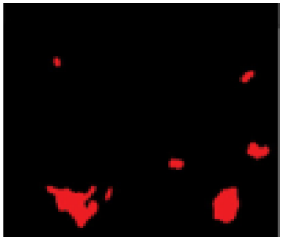
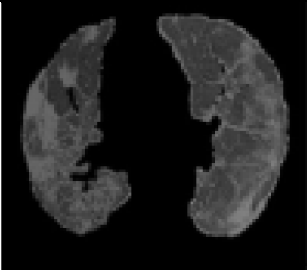
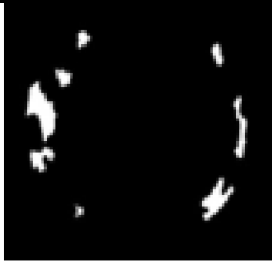
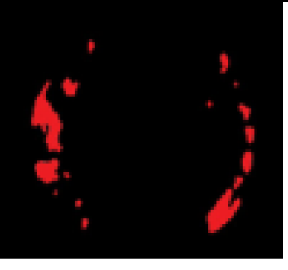
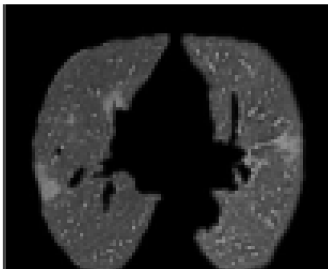
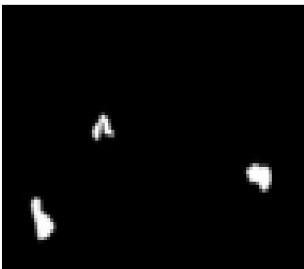
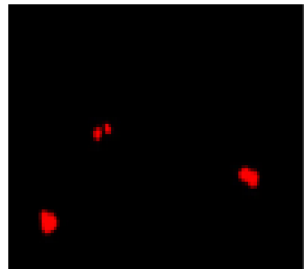
Original image	Ground truth	Segmented results
		
		
		
		
		

Table 3 Dissimilar region dimension accuracy analysis

Local patch size	Semi-global patch size	Lesion segmentation based on dice value (%)
12×12	40×40	25
12×12	50×50	33
12×12	80×80	43
12×12	70×70	42
12×12	60×60	35
17×17	80×80	81
17×17	70×70	74
17×17	60×60	73
17×17	50×50	70
17×17	40×40	62
22×22	80×80	91
22×22	70×70	89
22×22	60×60	82
22×22	50×50	77
22×22	40×40	75
26×26	80×80	88
26×26	70×70	90
26×26	60×60	93
26×26	50×50	75
26×26	40×40	58

$$R_{VD}(N_{S1}, N_{S2}) = \left(\frac{N_{S1} - N_{S2}}{N_{S2}} \right) \times 100\% \tag{15}$$

where the segmentation outputs of proposed and ground truth image are N_{s1} and N_{s2} . The segmentation result of the proposed and ground truth output is $C_{N_{s1}}$ and $C_{N_{s2}}$.

Performance Evaluation

Table 3 expresses the dissimilar region dimension accuracy analysis. To recognize inflammation in the tiny air sacs, apply local patches with the scar tissues and analogous touching textures to deliver details by employing

Table 4 Previous result of segmentation results

Techniques	Measures for evaluation		
	V (%)	A_{SD} (mm)	M_{SD} (mm)
ADECO-CNN	8.3 ± 5.3	5.1 ± 1.2	16.5 ± 8.2
PNN	8.9 ± 0.3	6.3 ± 7.3	21.2 ± 2.2
MT-DL	1.1 ± 1.5	5.3 ± 8.2	23.34 ± 9.3
Inf-Net	11.4 ± 2.1	5.1 ± 0.3	20.5 ± 6.4
Proposed method	5.4 ± 1.1	2.7 ± 0.3	7.2 ± 6.3

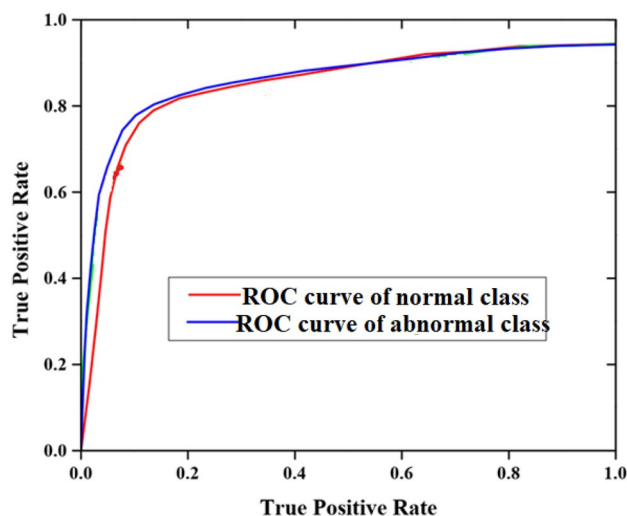


Fig. 6 ROC cure performance analysis

semi-global patches. From the global windows, the extracted information is based on the inflammation detection results. In the outcome of our approach, the local patches and the semi-global patches effect are employed.

Table 4 explains the previous segmentation outputs briefly. This investigation was performed among various methods, such as ADECO-CNN [14], PNN [18], MT-DL [21], Inf-Net [22], and the proposed method. The proposed method offers more volume overlap error, average surface distance, and maximum surface distance results than existing methods. The proposed method provides good results than other existing techniques. Figure 6 explains the normal and abnormal lung infection results based on the ROC curve.

Figure 7 expresses the comparative result of precision. The ADECO-CNN [14], PNN [18], MT-DL [21], Inf-Net [22], and the proposed method are used to validate the precision results. The ADECO-CNN, PNN, MT-DL, Inf-Net, and proposed method provided 80%, 83%, 84%, 86%, and 90% precision results. Compared to the previous methods, the proposed method provided better precision results.

The state-of-art result of the segmentation of different measures is depicted in Table 5. The ADECO-CNN, PNN, MT-DL, and Inf-Net are the existing methods. The measure results of root mean square symmetric surface distance and relative volume difference results. The proposed method accomplished good and more optimal results than existing methods like ADECO-CNN, PNN, MT-DL, and Inf-Net.

Figure 8 depicts the recall comparison result. The recall results are validated using the ADECO-CNN, PNN, MT-DL, Inf-Net, and suggested technique. ADECO-CNN, PNN, MT-DL, Inf-Net, and the proposed approach provided recall results of 80%, 86%, 90%, 92%, and 94%, respectively. The new method offered more incredible recall results when compared to the previous methods.

Fig. 7 Comparative result of precision

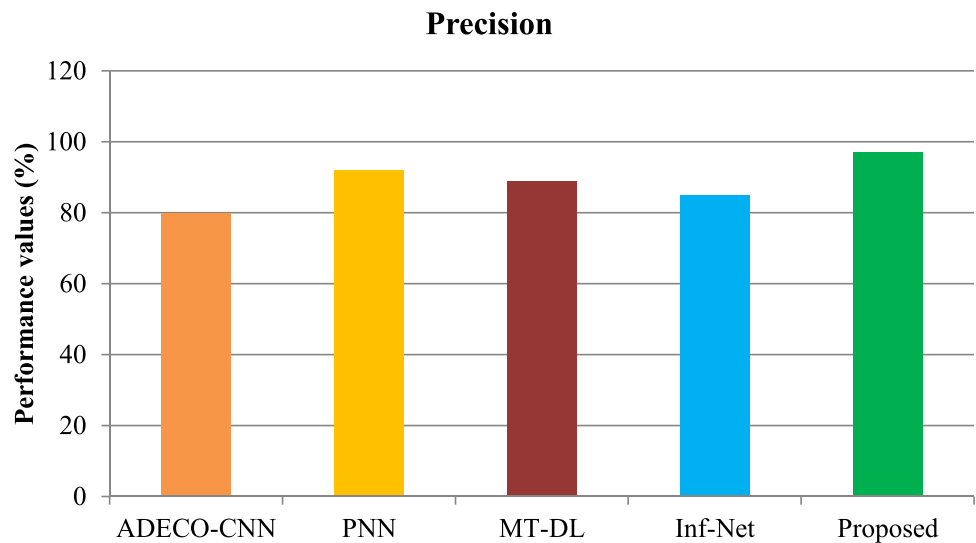


Table 5 Previous result of segmentation of different measures

Techniques	Measures for evaluation	
	R_{MSD} (mm)	R_{VD} (mm)
ADECO-CNN	5.2 ± 1.5	7.8 ± 0.3
PNN	4.7 ± 2.1	-4.2 ± 8.2
MT-DL	5.8 ± 5.3	5.8 ± 7.3
Inf-Net	5.5 ± 0.3	-4.7 ± 1.2
Proposed method	3.4 ± 0.3	3.7 ± 1.3

Figure 9 illustrates the comparative result of the F -score. The ADECO-CNN, PNN, MT-DL, Inf-Net, and the proposed method validate the F -score results. The

ADECO-CNN, PNN, MT-DL, Inf-Net, and proposed method provided 80%, 90%, 92%, 94%, and 95% F -score outputs. While comparing with the previous methods, our approach provided maximized F -score results.

Discussion

The proposed SegNet-CNN-based IGWO model performed well, achieving the best recall, F -measure, precision, and AUC results. As a result, the developed scheme eliminated the training flaws at the outset. Then, extract the features based on the aspect terms of the COVID-19 lung-affected parts. Furthermore, segmentation is performed in the classification layer when mask images are used. As a result, the

Fig. 8 Comparative result of a recall

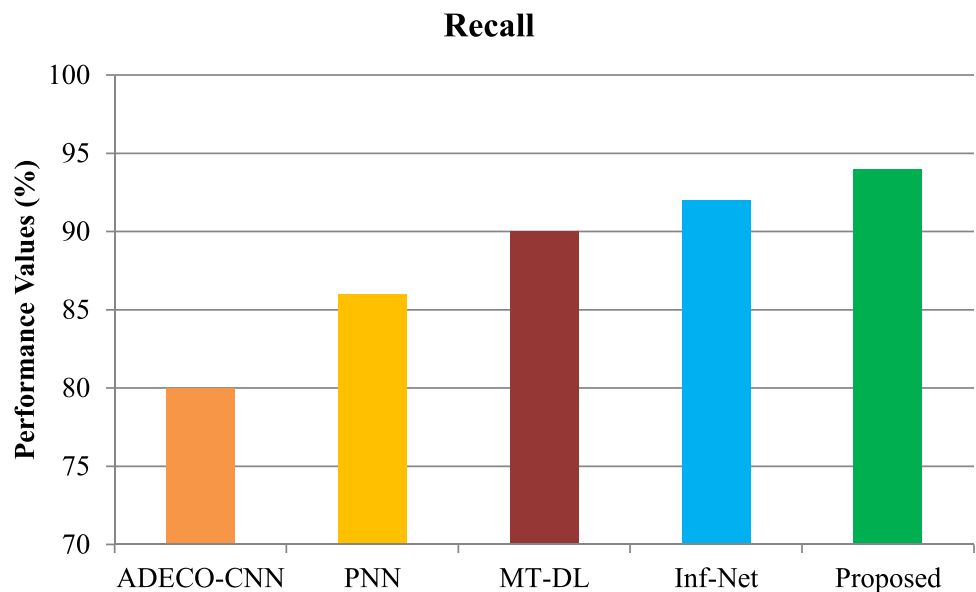
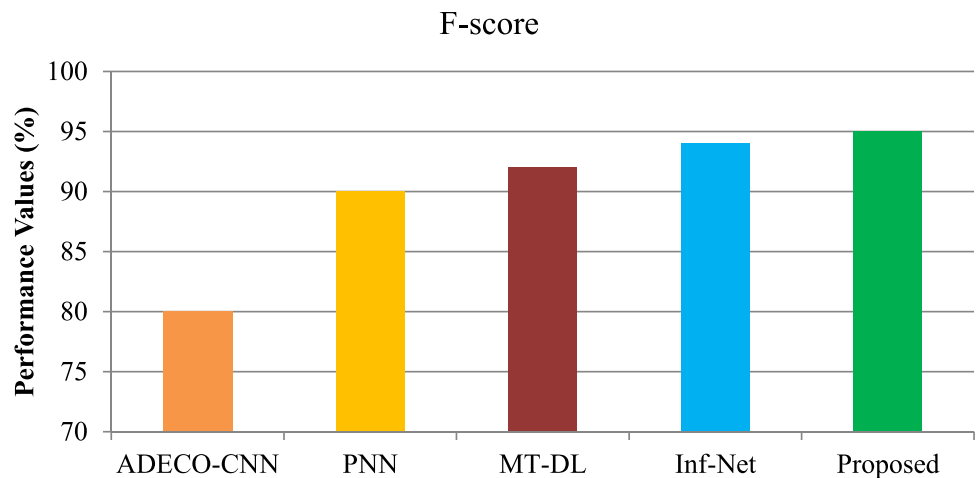


Fig. 9 Comparative result of *F*-score**Table 6** Overall performance metrics

Methods	Performance assessment with key metrics		
	Precision	Recall	<i>F</i> -score
ADECO-CNN	80	80	80
PNN	83	86	90
MT-DL	84	90	92
Inf-Net	86	92	94
Proposed method	90	94	95

developed SegNet-CNN-based IGWO technique improves the performance of segmented COVID-19-infected lungs.

The outstanding performance measures comparisons are computed in Table 6, and the proposed SegNet-CNN-based IGWO has obtained the best results in all parameter validation. Furthermore, they achieved 90% precision, 94% recall, and 95% *F*-score. As a result, the proposed SegNet-CNN-based IGWO robustness is confirmed, and it can segment COVID-19 lungs-affected parts.

Conclusion

The work in this article is based on the novel approach known as the SegNet-based CNN-IGWO algorithm for the segmentation of COVID-19-infected lung parts. After collecting the dataset, the images were normalized to remove the unwanted noises caused due to the electronic equipment, surroundings, etc. The normalization is carried out using the Z-score normalization approach. Then, the normalized images were segmented using the proposed SegNet-IGWO approach. This approach effectively segmented the images. Experimental analysis shows that the proposed approach

segmented the images more accurately than the other existing approaches. Furthermore, the evaluation metrics such as *F*1-score, precision, recall, and dice index were analyzed and compared with previous works such as ADECO-CNN, PNN, MT-DL, and Inf-Net. Our proposed work performs better than the other approaches. The proposed work provides a 90% better precision and a 95% better result for *F*-score. Additional data for training and more labeled data for multi-class segmentation can be used to improve the outcomes which constitute our future research.

Availability of Data and Material Data sharing is not applicable to this article as no new data were created or analyzed in this study.

Code Availability Not applicable.

Declarations

Consent to Participate Informed consent does not apply as this was a retrospective review with no identifying patient information.

Consent for Publication Not applicable.

Conflict of Interest The authors declare no competing interests.

Human and Animal Rights This article does not contain any studies with human or animal subjects performed by any of the authors.

References

1. Perlman S. Another decade, another coronavirus. *N Engl J Med*. 2020;382(8):760–2.
2. He F, Deng Y, Li W. Coronavirus disease 2019: what we know? *J Med Virol*. 2020;92(7):719–25.
3. World Health Organization. Coronavirus disease 2019 (COVID-19): situation report. 2020;73.
4. Zu ZY, Jiang MD, Xu PP, Chen W, Ni QQ, Lu GM, Zhang LJ. Coronavirus disease 2019 (COVID-19): a perspective from China. *Radiology*. 2020;296(2):E15–25.

5. Allam Z, Dey G, Jones DS. Artificial intelligence (AI) provided early detection of the coronavirus (COVID-19) in China and will influence future urban health policy internationally. *Ai*. 2020;1(2):156–65.
6. Pham QV, Nguyen DC, Huynh-The T, Hwang WJ, Pathirana PN. Artificial intelligence (AI) and big data for coronavirus (COVID-19) pandemic: a survey on the state-of-the-arts. *IEEE Access*. 2020;8:130820.
7. Gozes O, Frid-Adar M, Sagie N, Zhang H, Ji W, Greenspan H. Coronavirus detection and analysis on chest ct with deep learning. 2020. arXiv preprint: <http://arxiv.org/abs/2004.02640>.
8. Ghoshal B, Tucker A. Estimating uncertainty and interpretability in deep learning for coronavirus (COVID-19) detection. 2020. arXiv preprint: <http://arxiv.org/abs/2003.10769>.
9. Saood A, Hatem I. COVID-19 lung CT image segmentation using deep learning methods: U-Net versus SegNet. *BMC Med Imaging*. 2021;21(1):1–10.
10. Mahdy LN, Ezzat KA, Elmousalami HH, Ella HA, Hassanien AE. Automatic x-ray covid-19 lung image classification system based on multi-level thresholding and support vector machine. 2020. *MedRxiv*.
11. Yan Q, Wang B, Gong D, Luo C, Zhao W, Shen J, Shi Q, Jin S, Zhang L, You Z. COVID-19 chest CT image segmentation--a deep convolutional neural network solution. 2020. arXiv preprint: <http://arxiv.org/abs/2004.10987>.
12. Ranjbarzadeh R, Jafarzadeh Ghouschi S, Bendechache M, Amirabadi A, Ab Rahman MN, Baseri Saadi S, Aghamohammadi A, Kooshki Forooshani M. Lung infection segmentation for COVID-19 pneumonia based on a cascade convolutional network from CT images. *BioMed Res Int*. 2021.
13. Singh D, Kumar V, Yadav V, Kaur M. Deep neural network-based screening model for COVID-19-infected patients using chest X-ray images. *Int J Pattern Recognit Artif Intell*. 2021;35(03):2151004.
14. Castiglione A, Vijayakumar P, Nappi M, Sadiq S, Umer M. Covid-19: Automatic detection of the novel coronavirus disease from ct images using an optimized convolutional neural network. *IEEE Trans Industr Inf*. 2021;17(9):6480–8.
15. Castiglione A, Umer M, Sadiq S, Obaidat MS, Vijayakumar P. The role of internet of things to control the outbreak of COVID-19 pandemic. *IEEE Internet Things J*. 2021;8(21):16072–82.
16. Vahdat S, Kamal M, Afzali-Kusha A, Pedram M. LATIM: loading-aware offline training method for inverter-based memristive neural networks. *IEEE Trans Circuits Syst II Express Briefs*. 2021;68(10):3346–50.
17. Kaiser MS, Mahmud M, Noor MBT, Zenia NZ, Al Mamun S, Mahmud KA, Azad S, Aradhya VM, Stephan P, Stephan T, Kannan R. iWork-Safe: towards healthy workplaces during COVID-19 with an intelligent pHealth App for industrial settings. *Ieee Access*. 2021;9:13814–28.
18. Aradhya VM, Mahmud M, Chowdhury M, Guru DS, Kaiser MS, Azad S. Learning through one shot: a phase by phase approach for COVID-19 chest X-ray classification. In 2020 IEEE-EMBS Conference on Biomedical Engineering and Sciences (IECBES) IEEE. 2021;241–44.
19. Mahmud T, Alam MJ, Chowdhury S, Ali SN, Rahman MM, Fattah SA, Saquib M. CovTANet: a hybrid tri-level attention-based network for lesion segmentation, diagnosis, and severity prediction of COVID-19 chest CT scans. *IEEE Trans Industr Inf*. 2020;17(9):6489–98.
20. Mahmud T, Rahman MA, Fattah SA, Kung SY. CovSegNet: a multi encoder–decoder architecture for improved lesion segmentation of COVID-19 chest CT scans. *IEEE Trans Artif Intell*. 2021;2(3):283–97.
21. Elharrouss O, Subramanian N, Al-Maadeed S. An encoder–decoder-based method for segmentation of COVID-19 lung infection in CT images. *SN Comput Sci*. 2022;3(1):1–12.
22. Fan DP, Zhou T, Ji GP, Zhou Y, Chen G, Fu H, Shen J, Shao L. Inf-net: automatic covid-19 lung infection segmentation from ct images. *IEEE Trans Med Imaging*. 2020;39(8):2626–37.
23. Chvetsov AV, Paige SL. The influence of CT image noise on proton range calculation in radiotherapy planning. *Phys Med Biol*. 2010;55(6):N141.
24. Patro S, Sahu KK. Normalization: a preprocessing stage. 2015. arXiv preprint:<http://arxiv.org/abs/1503.06462>.
25. Gonçalves DN, de Moares Weber VA, Pistori JGB, da Costa Gomes R, de Araujo AV, Pereira MF, Gonçalves WN, Pistori H. Carcass image segmentation using CNN-based methods. *Inf Process Agric*. 2020.
26. Tian Z, Shen C, Wang X, Chen H. Boxinst: high-performance instance segmentation with box annotations. In *Proceedings of the IEEE/CVF Conference on Computer Vision and Pattern Recognition*. 2021;5443–52.
27. Maqsood M, Nazir F, Khan U, Aadil F, Jamal H, Mehmood I, Song OY. Transfer learning assisted classification and detection of Alzheimer’s disease stages using 3D MRI scans. *Sensors*. 2019;19(11):2645.
28. Albahli S, Nida N, Irtaza A, Yousaf MH, Mahmood MT. Melanoma lesion detection and segmentation using YOLOv4-DarkNet and active contour. *IEEE Access*. 2020;8:198403–14.
29. Qassim H, Verma A, Feinzimer D. Compressed residual-VGG16 CNN model for big data places image recognition. In *2018 IEEE 8th Annual Computing and Communication Workshop and Conference (CCWC)*. IEEE. 2018;169–75.
30. Carvalho T, De Rezende ER, Alves MT, Balieiro FK, Sovat RB. Exposing computer generated images by eye’s region classification via transfer learning of VGG19 CNN. In *2017 IEEE International Conference on Machine Learning and Applications (ICMLA)*. IEEE. 2017;866–70.
31. Theckedath D, Sedamkar RR. Detecting affect states using VGG16, ResNet50 and SE-ResNet50 networks. *SN Comput Sci*. 2020;1(2):1–7.
32. Ketkar N. Stochastic gradient descent. In *Deep Learning with Python*. Apress Berkeley CA. 2017;113–32.
33. Nadimi-Shahraki MH, Taghian S, Mirjalili S. An improved grey wolf optimizer for solving engineering problems. *Expert Syst Appl*. 2021;166:113917.
34. Gupta S, Deep K. A novel random walk grey wolf optimizer. *Swarm Evol Comput*. 2019;44:101–12.
35. Teixeira LO, Pereira RM, Bertolini D, Oliveira LS, Nanni L, Cavalcanti GD, Costa YM. Impact of lung segmentation on the diagnosis and explanation of COVID-19 in chest X-ray images. *Sensors*. 2021;21(21):7116.
36. Chen C, Xiao R, Zhang T, Lu Y, Guo X, Wang J, Chen H, Wang Z. Pathological lung segmentation in chest CT images based on improved random walker. *Comput Methods Programs Biomed*. 2021;200:105864.
37. Yao Q, Xiao L, Liu P, Zhou SK. Label-free segmentation of COVID-19 lesions in lung CT. *IEEE Trans Med Imaging*. 2021;40(10):2808–19.
38. Saeedizadeh N, Minaee S, Kafieh R, Yazdani S, Sonka M. COVID TV-Unet: segmenting COVID-19 chest CT images using connectivity imposed Unet. *Computer Methods and Programs in Biomedicine Update*. 2021;1:100007.
39. Gozes O, Frid-Adar M, Greenspan H, Browning PD, Zhang H, Ji W, Bernheim A, Siegel E. Rapid ai development cycle for the coronavirus (covid-19) pandemic: initial results for automated detection & patient monitoring using deep learning ct image analysis. 2020. arXiv preprint: <http://arxiv.org/abs/2003.05037>.

Publisher’s Note Springer Nature remains neutral with regard to jurisdictional claims in published maps and institutional affiliations.

Springer Nature or its licensor (e.g. a society or other partner) holds exclusive rights to this article under a publishing agreement with the author(s) or other rightsholder(s); author self-archiving of the accepted manuscript version of this article is solely governed by the terms of such publishing agreement and applicable law.